Du *et al. BMC Oral Health* (2025) 25:42
https://doi.org/10.1186/s12903-024-05345-9

BMC Oral Health

RESEARCH

Open Access

Feasibility of occlusal plane in predicting the changes in anteroposterior mandibular position: a comprehensive analysis using deep learning-based three-dimensional models

Bingran Du[1†], Kaichen Li[2†], Zhiling Shen[3], Yihang Cheng[3], Jiayan Yu[3], Yaopeng Pan[1], Ziyan Huang[3], Fei Hu[3], Xiaohui Rausch-Fan[4], Yuanpeng Zhu[2*] and Xueyang Zhang[1,3*]

Abstract

Background A comprehensive analysis of the occlusal plane (OP) inclination in predicting anteroposterior mandibular position (APMP) changes is still lacking. This study aimed to analyse the relationships between inclinations of different OPs and APMP metrics and explore the feasibility of OP inclination in predicting changes in APMP.

Methods Overall, 115 three-dimensional (3D) models were reconstructed using deep learning-based cone-beam computed tomography (CBCT) segmentation, and their accuracy in supporting cusps was compared with that of intraoral scanning models. The anatomical landmarks of seven OPs and three APMP metrics were identified, and their values were measured on the sagittal reference plane. The receiver operating characteristic curves of inclinations of seven OPs in distinguishing different anteroposterior skeletal patterns and correlations between inclinations of these OPs and APMP metrics were calculated and compared. For the OP inclination wit*h* the highest area under the curve (AUC) values and correlation coefficients, the regression models between this OP inclination and APMP metrics were further calculated.

Results The deviations in supporting cusps between deep learning-based and intraoral scanning models were <0.300 mm. The improved functional OP (IFOP) inclination could distinguish different skeletal classification determinations ($AUC_{\text{Class I } VS \text{ Class II}} = 0.693$, $AUC_{\text{Class I } VS \text{ Class III}} = 0.763$, $AUC_{\text{Class II } VS \text{ Class III}} = 0.899$, all P values < 0.01) and the AUC value in skeletal Classes II and III determination was statistically higher than the inclinations of other OPs (all P values < 0.01). Moreover, the IFOP inclination showed statistical correlations with APMP metrics ($r_{APDI} = -0.557$, $r_{ANB} = 0.543$, $r_{AF-BF} = 0.731$, all P values < 0.001) and had the highest correlation coefficients among all OP inclinations (all P

†Bingran Du and Kaichen Li contributed equally to this work as first authors.

*Correspondence:
Yuanpeng Zhu
zhuyuanpeng@csu.edu.cn
Xueyang Zhang
zxy123@smu.edu.cn

Full list of author information is available at the end of the article

values < 0.05). The regression analysis models of IFOP inclination and APMP metrics were $y_{APDI} = -0.917x + 91.144$, $y_{ANB} = 0.395x + 0.292$, and $y_{AF-BF} = 0.738x - 2.331$.

Conclusions Constructing the OP using deep learning-based 3D models from CBCT data is feasible. IFOP inclination could be used in predicting the APMP changes. A steeper IFOP inclination corresponded to a more retrognathic mandibular posture.

Keywords Deep learning, Occlusal plane, Anteroposterior mandibular position

Background

The three-dimensional (3D) spatial position of the mandible, particularly its anteroposterior position, is crucial in human facial growth [1, 2]. An imbalance in the anteroposterior mandibular position (APMP) can lead to poor oral function [3] and concerns regarding facial aesthetics [4], which impair social and psychological quality of life [5]. With the advancement of technology, camouflage orthodontic treatment has rapidly progressed [6]. For adults with APMP imbalances who refuse the orthognathic surgery due to the economic and psychological burdens, camouflage orthodontic treatment ca.*n* be used to improve the facial aesthetics and oral function by promoting favorable mandibular rotation [7, 8].

Considering the complexity of the regulatory mechanism of orthodontics-induced mandibular rotation, a parameter in predicting changes in APMP is needed for orthodontists to conduct effective and efficient treatment. The occlusal plane (OP) refers to an imaginary surface at the level of occlusion [9]. Since the 1940s, numerous scholars have observed a fact that individuals with retrognathic or prognathic mandibular posture tend to show steeper or flatter OP [10–13], which indicates that OP inclination may be an important parameter in predicting APMP. However, this finding has not been consistently observed in all clinical orthodontic practices [14, 15], reflecting the uncertainty regarding the OP inclination as a predictive parameter for APMP. Therefore, further analysis is required to explore the relationship between OP inclination and APMP.

The inaccurate representation of various OPs may be the most limiting factor in analysing the relationship between OP inclination and APMP. Traditionally, many OPs used in clinical practice are represented by straight lines on two-dimensional radiographs, which are prone to inaccuracies due to landmark errors and image magnification [16]. Although cone-beam computed tomography (CBCT) can address these issues [17], achieving accurate and reliable representations of some OPs in maximum intercuspation remains challenging. Therefore, it is crucial to explore a more accurate method for representing various OPs in clarifying the relationship between OP inclination and APMP.

Recently, CBCT imaging-based deep neural networks have demonstrated high performance in segmenting teeth, alveolar bone, and other structures, significantly aiding clinical diagnostics, treatment, and evaluation [18–20]. Given the remarkable achievements of deep learning in the field of dentistry, the precise representation of OP in 3D models using deep learning-based CBCT segmentation would be possible.

This study aimed to analyse the relationships between the inclinations of different OPs and APMP metrics using deep learning-based 3D models and explore the feasibility of OP inclination used in predicting the changes in APMP. We hypothesised that there are differences in the relationships between the inclinations of various OPs and APMP metrics and that the inclination of specific OP can be used as a parameter in predicting changes in APMP.

Methods

CBCT images of 115 patients (63 females and 52 males, age range of 18–39 years) were obtained from our institution using NewTom VGi (Cefla, Imola, Italy). CBCT images were captured by the same technician under consistent settings, with a tube voltage of 110 kV and a current of 3 mA. The CBCT scans were taken with the patients seated, with their heads positioned according to three light beams. The upper horizontal light beam passed through the subnasale, the lower horizontal light beam passed through the anterior-most point on the chin, and the sagittal light beam was aligned with the midline of the patient's face. During the scanning, the patients were required to remain still and refrain from swallowing. All patients provided informed consents to participate in this study, and the study was approved by the ethics review board of our institution (Approval No.: KYLS20220913).

The inclusion criteria were as follows: (1) fully erupted permanent dentition; (2) no previous orthodontic treatment; (3) no bone defects, severe mandibular skeletal asymmetry (menton deviation > 4 mm) [21], or other craniomaxillofacial deformities; and (4) no tooth loss, severe tooth wear, dental prosthesis, or posterior crossbite. All included patients were categorised into skeletal Classes I, II, and III based on the results of the majority of the APMP metrics, including the anteroposterior dysplasia indicator (APDI) [22], ANB angle [23], and AF-BF distance [24]. In cases where all metrics for diagnosing anteroposterior skeletal classes did not align, a decision was made by an orthodontist based on radiographic evaluation and clinical judgment [25]. The final classification of the patients resulted in the following groups: skeletal Class I (n=30), Class II (n=51), and Class III (n=34).

CBCT data were automatically segmented using deep learning technology (3D U-Net Convolution Neural Network) and reconstructed into 3D models in Remebot Jaw Motion Analyser (Beijing Ruiyibo Technology Co., Ltd., Beijing, China). Based on these 3D models, 13 landmarks on craniofacial hard tissues (Table 1) [26–29] and 70 landmarks on tooth cusps (Fig. 1), respectively, were marked by a trained resident using the 3D marking method that incorporates multi-planar reformations [30]. Subsequently, three reference planes were constructed in Geomagic Studio 2014 (3D Systems Inc., Rock Hill, SC, USA), including the Frankfort horizontal plane (FHP) [27], the sagittal reference plane (SRP) [26], and the coronal reference plane (CRP) (Fig. 2). The coordinates of corresponding landmarks and the reference plane information were then imported into MATLAB (MathWorks Inc., Natick, MA, USA), where the three APMP metrics and the inclinations of seven OPs were calculated.

The APMP metrics included the APDI, ANB angle, and AF-BF distance, which were calculated as angular values or linear distances formed by the landmarks projected onto the SRP (Table 2; Fig. 3). OPs included the posterior OP [31], anterior OP [31], bisected OP [32], maxillary OP [33], mandibular OP [33], and functional OP (FOP) [34], which have been described in previous studies, as well as the improved FOP (IFOP), which we created according to the definition that FOP divides posterior occlusal contacts [35]. OP inclination was defined as the angle between the FHP and the sagittal projected line of OP. A negative value indicated that the projected line was angled above the FHP, whereas a positive value showed that the lines were angled below the FHP. The sagittal projected line was generated by projecting the corresponding cusps onto the SRP using the minimum distance method (Table 3; Fig. 4). The formula is as follows:

$$E(A,\ B,\ C)\ =\sum\nolimits_{i=1}^{n}(A*\ x_i+B*\ y_i+c)^2$$

where $E(A,\ B,\ C)$ is the error function representing the sum of squared distances; n is the total number of cusps; (x_i, y_i) are the coordinates of the ith cusps; $A, B,$ and C are parameters of the line equation $Ax\ +\ By\ +\ C\ =\ 0$; and $A*x_i+B*y_i+C$ represents the signed distance from the ith cusp to the line. The objective of this analysis was to determine the values of $A, B,$ and C that minimise the sum of squared distances.

Before analysing the relationship between the inclinations of different OPs and APMP metrics, Trios 3 scanner-acquired intraoral scanning models (3Shape, Copenhagen, Denmark) of 25 randomly selected patients among 115 patients were collected and imported into Geomagic Control X v2020.1.1 (3D Systems Inc.) to evaluate the accuracy of supporting teeth cusps on deep learning-based 3D models. Deviations between deep learning-based and intraoral scanning 3D models were subsequently calculated using the following parameters: overall positive deviation, overall negative deviation, and absolute deviation of supporting cusps.

In this study, 60 samples were randomly selected 2 weeks after the initial landmarking and were re-landmarked by another resident to evaluate inter-examiner reliability. The resident also received standardised training to ensure consistency in the landmarking process.

Statistical analysis

Statistical analyses were performed using Microsoft Excel (Microsoft Corp., Redmond, WA, USA) and IBM SPSS for Windows, version 27.0 (IBM Corp., Armonk, NY, USA). P values < 0.05 were considered statistically

Table 1 Landmarks on craniofacial hard tissue

Landmark	Abbreviation	Definition
Nasion	N	Medial (and upper) point of the frontonasal suture[26]
Sella	S	Central point of the sella[26]
Anterior nasal spine	ANS	Medial and most anterior point of the nasal spine [26]
Posterior nasal spine	PNS	Medial and most distal point of the osseous palate [26]
Orbitale	Or-L/Or-R	The lowest point of the orbital rim L/R [26]
Pogonion	Pog	Medial and most anterior point of the mandible [26]
Internal Acoustic Foramen	IAF-L/IAF-R	The most lateral point of the internal auditory meatusat the skull base L/R[27]
Incisive foramen	IF	Anteroposterior and me-diolateral center of the incisive foramen [28]
Basion	Ba	Middorsal point of the anterior margin of the foramen magnum on the basilar part of the occipital bone [28]
A-point	A	The deepest bony point on the contour of the premaxilla below ANS [29]
B-Point	B	The deepest bony point on the contour of the mandible above the Pog [29]

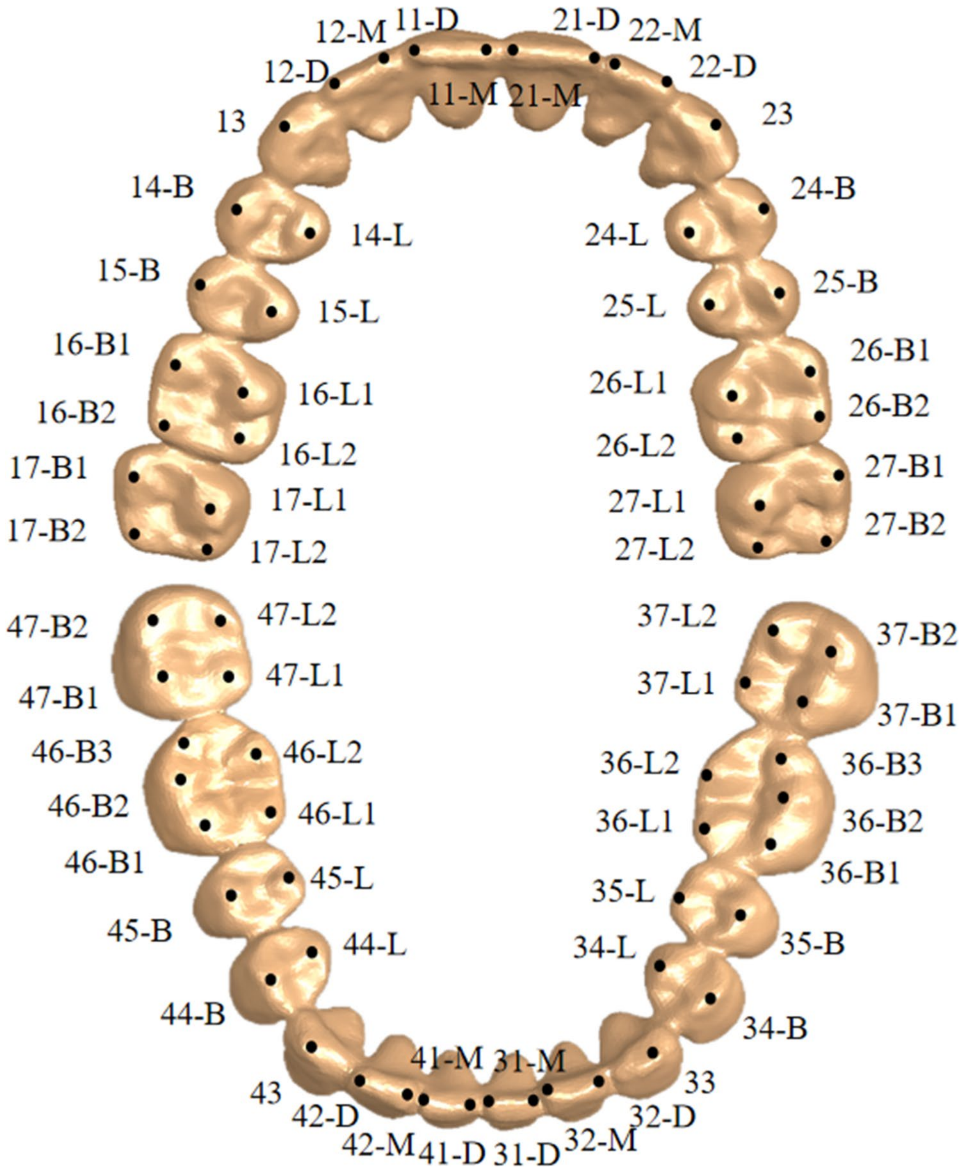

Fig. 1 Landmarks on tooth cusps

significant. The Shapiro–Wilk test was used to assess the normality of the data.

Sex-based differences were determined using the Mann–Whitney U test and independent-samples t-test for non-normally and normally distributed data, respectively. Receiver operating characteristic (ROC) curve analysis was used to test the ability of the inclinations of different OPs to distinguish various anteroposterior skeletal patterns. The correlations between the inclinations of different OPs and APMP metrics were calculated and compared using Spearman's rank correlation analysis and the method proposed by Meng et al. [36]. Moreover, the simple linear regression models were calculated to explore the precise relationship between the inclination of specific OP and each APMP metric. The intraclass correlation coefficient (ICC) [37] and measurement errors (Dahlberg's formula) [38] of landmarks on craniofacial hard tissues and the cusps were calculated to assess the inter-examiner reliability.

Based on our preliminary research and clinical perspective, this study concentrated on examining the correlation between the IFOP inclination and APMP metrics, and the correlation coefficient was conservatively estimated to be 0.3. PASS15.0 (NCSS, LLC. Kaysville, UT, USA) software was used to calculate the sample size, with a type I error (α) of 0.05 and a power of 0.9 for hypothesis testing. This analysis yielded a required sample size of 112. Therefore, the CBCT images of 115 patients collected for this investigation were deemed sufficient.

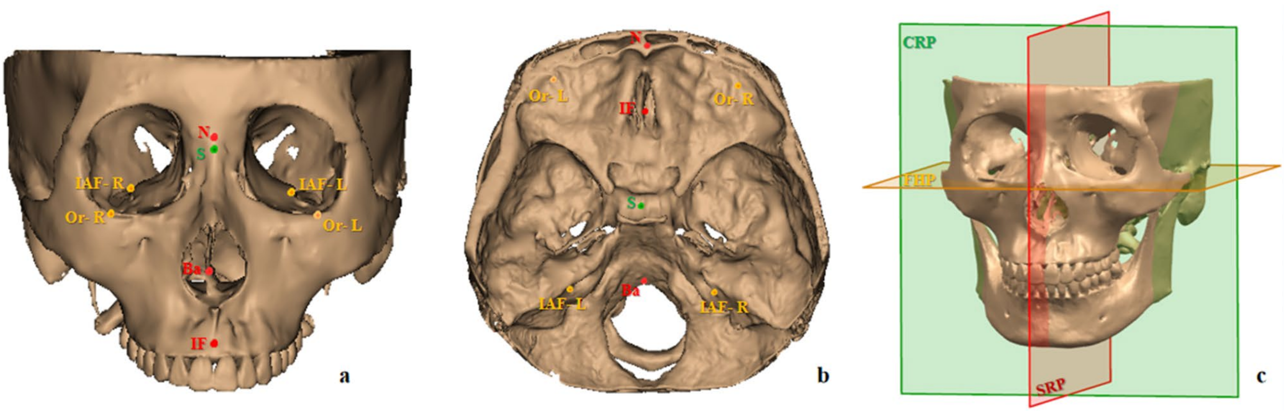

Fig. 2 Construction of reference planes. **a**: Front view of relevant anatomical landmarks. **b**: Top view of relevant anatomical landmarks. **c**: Three reference planes—SRP, sagittal reference plane (plane through N, Ba, and IF); FHP, Frankfort horizontal plane (plane perpendicular to the SRP and passing through two points: the midpoint of IAF-L and IAF-R and the midpoint of Or-L and Or-R); and CRP, coronal reference plane (plane passing through S and perpendicular to the SRP and FHP)

Table 2 Metrics of APMP

Metrics	Definition
APDI (°)	NP-FH ± NP-AB ± PP-FH. NP-FH, the angle made by the the N-Pog* line and FHP; NP-AB, the angle made by the the N-Pog* line and A*-B* line; PP-FH, the angle made by the the ANS*-PNS* line and FHP;
ANB (°)	The angle made by N-A* line and N-B* line
AF-BF (mm)	The linear distance between points A* and B* projected onto the FHP

*Corresponding points projected onto the sagittal reference plane (SRP)

Results

The values of overall positive deviation, overall negative deviation, and absolute deviation of supporting cusps between deep learning-based and intraoral scanning 3D models were 0.191 (0.095), -0.200 (0.103), and 0.231 (0.163) mm, respectively. Considering the clinically acceptable error (a threshold of <0.300 mm) [39], the accuracy of supporting cusps on deep learning-based 3D models was acceptable.

The evaluation of the reliability of the measured landmarks revealed that the Dahlberg errors *o*f the coordinate values of landmarks on tooth cusps (Tx, Ty, and Tz) were 0.529, 0.776, and 0.503 mm, respectively, and those of landmarks on craniofacial hard tissues (Cx, Cy, and Cz) were 0.935, 0.814, and 0.932 mm, respectively. Furthermore, the ICC scores of measured landmarks were all >0.800, indicating a good level of reliability.

Given that no statistically significant differences were observed between sexes (all P values > 0.05), the evaluations were conducted on pooled data without distinguishing based on sex. The ability test results of inclinations of seven OPs in distinguishing different anteroposterior skeletal patterns are shown in Fig. 5. In distinguishing skeletal Classes II and III, the area under the curve (AUC) value of IFOP inclination was 0.899, statistically higher than the values of inclinations of other OPs (all P values < 0.01). Although no statistical differences were observed between the AUC values of IFOP inclination and those of other OPs in distinguishing the Class I and the other two skeletal classes, the AUC values of IFOP inclination were the highest ($AUC_{\text{Class I } VS \text{ Class II}} = 0.693$; $AUC_{\text{Class I } VS \text{ Class III}} = 0.763$). Moreover, the correlations between the inclinations of different OPs and APMP metrics are presented in Table 4. As shown in Fig. 6, the correlation coefficients between IFOP inclination and APMP metrics were statistically different from those between the inclinations of other OPs and APMP metrics (all P values < 0.05).

To further analyse the relationships between IFOP inclination and APMP metrics, the regression model of IFOP inclination and APMP metrics were obtained, which are as follows: $y_{APDI} = -0.917x + 91.144$, $y_{ANB} = 0.395x + 0.292$, and $y_{AF-BF} = 0.738x - 2.331$. The corresponding R^2 values were 0.325, 0.311, and 0.474, respectively.

Discussion

In orthodontic practice, how to use the OP inclination to predict changes in APMP remains uncertain, which may lead to difficulty in establishing diagnosis, prognosis, and treatment plans for adults with mild to moderate APMP imbalance. To address this issue, our study aimed to analyse the relationship between OP inclination and APMP using deep learning-based 3D models, and to explore the feasibility of using OP inclination as a parameter for predicting the changes in APMP. The results from the ROC curve and correlation analyses of this study confirmed our hypothesis that the inclination of the IFOP formed by the contacting cusps of the posterior teeth could be used in predicting changes in APMP. Moreover, we found a

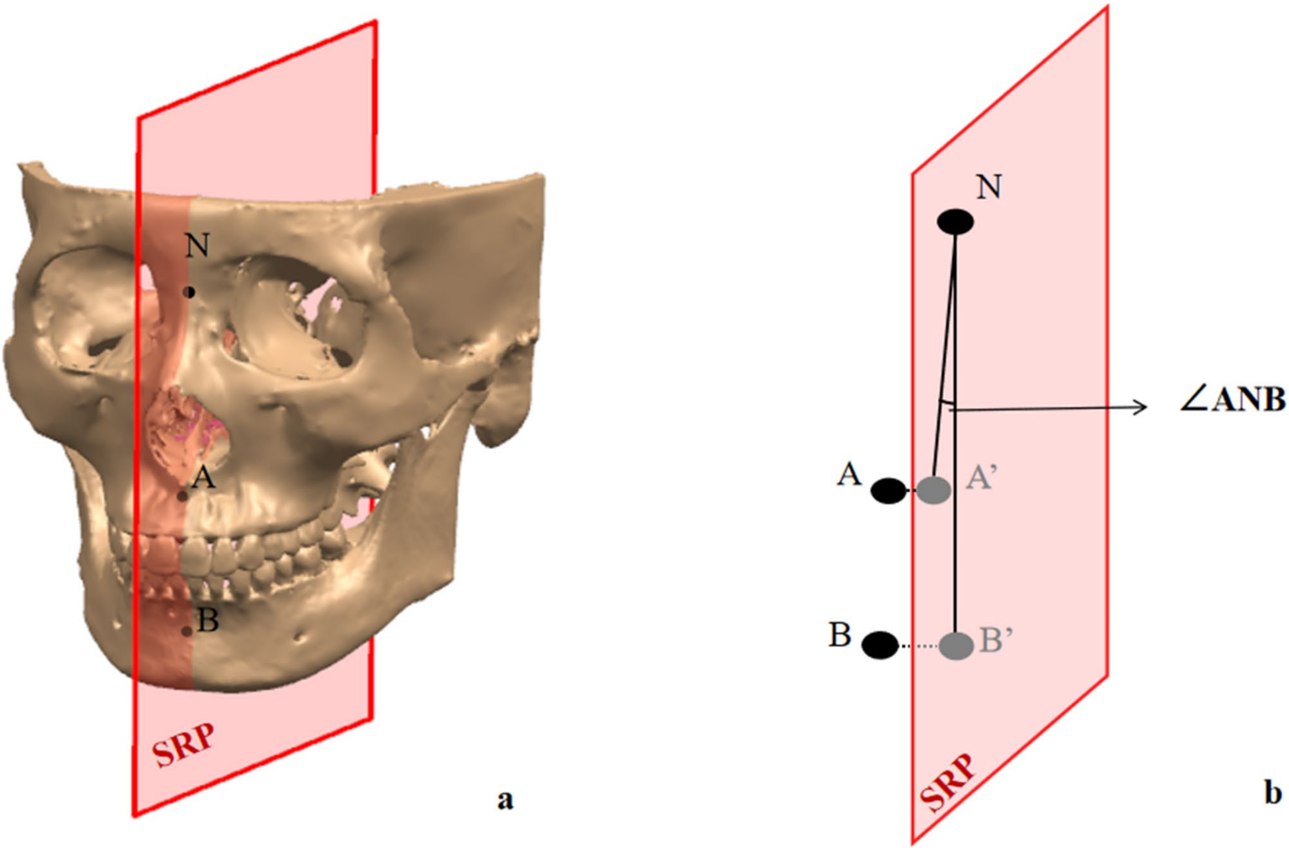

Fig. 3 Calculation of APMP metrics (with ANB as an example). **a**: Landmarks of the craniofacial hard tissue. **b**: Calculation of ANB on SRP. A' and B', the corresponding points of A and B projected onto the SRP. APMP, Anteroposterior mandibular position; SRP, Sagittal reference plane

Table 3 Corresponding cusps of occlusal planes (OPs)

OPs	Abbreviation	Corresponding cusps
Anterior OP	AOP	21-M, 15-B, 25-B
Posterior OP	POP	midpoint (15-B, 25-B), 17-B2, 27-B2
Bisected OP	BOP	midpoint (21-M, 31-M), midpoint (16-B2, 46-B2), midpoint (26-B2, 36-B2)
Maxillary OP	MxOP	21-M, 16-B1, 26-B1
Mandibular OP	MnOP	31-M, 36-B1, 46-B1
Functional OP	FOP	midpoint (14-B, 44-B), midpoint (24-B, 34-B), midpoint (15-B,45-B), midpoint (25-B, 35-B), midpoint (16-B1, 46-B1), midpoint (16-B2, 46-B2), midpoint (26-B1, 36-B1), midpoint (26-B2, 36-B2)
Improved functional OP	IFOP	14-B, 15-B, 16-B1, 16-B2, 17-B1, 17-B2; 24-B, 25-B, 26-B1, 26-B2, 27-B1, 27-B2; 14-L, 15-L, 16-L1, 16-L2 17-L1, 17-L2; 24-L, 25-L, 26-L1, 26-L2, 27-L1, 27-L2; 34-B, 35-B, 36-B1, 36-B2, 36-B3, 37-B1, 37-B2; 44-B, 45-B, 46-B1, 46-B2, 46-B3, 47-B1, 47-B2; 34-L, 35-L, 36-L1, 36-L2, 37-L1, 37-L2; 44-L, 45-L, 46-L1, 46-L2, 47-L1, 47-L2 (The tooth cusp tips mentioned without occlusal contacts in intercuspal position would be excluded.)

Note: midpoint (cusp tip 1, cusp tip 2) refers to the midpoint between cusp tip 1 and cusp tip 2

steeper IFOP inclination corresponded to a more retrognathic mandibular posture.

Accurate representation of OP is foundational for analysing the relationship between OP inclination and APMP. While intraoral scanning can accurately capture the occlusal surface of the tooth for better OP representation [40], its limitations in application and high management costs hinder the acquisition of sufficient samples [41]. Therefore, we opted for deep learning-based CBCT segmentation to create OP instead of intraoral scanning. Although this technology has been successfully applied in maxillofacial disease diagnosis [42], its feasibility in creating OPs has not been thoroughly explored. Our study demonstrated that deep learning-based CBCT segmentation could identify the supporting cusps of both upper and lower teeth, indicating its promising potential for OP construction.

Accurate evaluation of APMP is the key to analysing the relationship between OP inclination and APMP. Considering that no single measurement is currently accepted

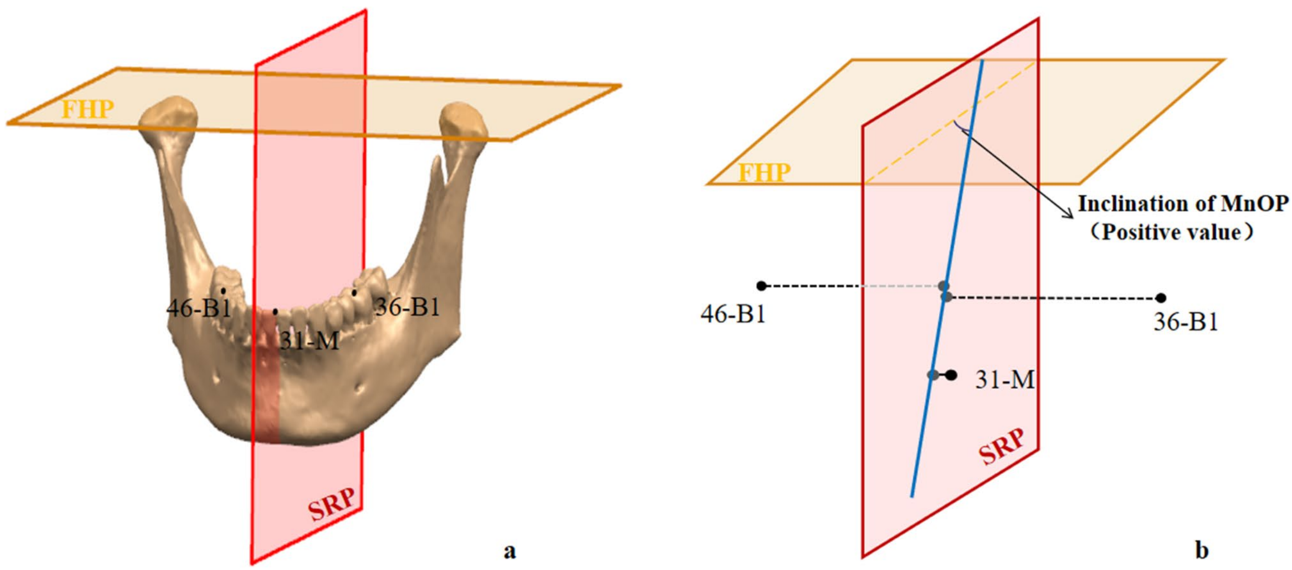

Fig. 4 Calculation of OP inclination (with MnOP as an example). **a**: Landmarks of cusps. **b**: Inclination of MnOP. Blue line, the sagittal projected line of MnOP. OP, Occlusal plane; MnOP, Mandibular occlusal plane

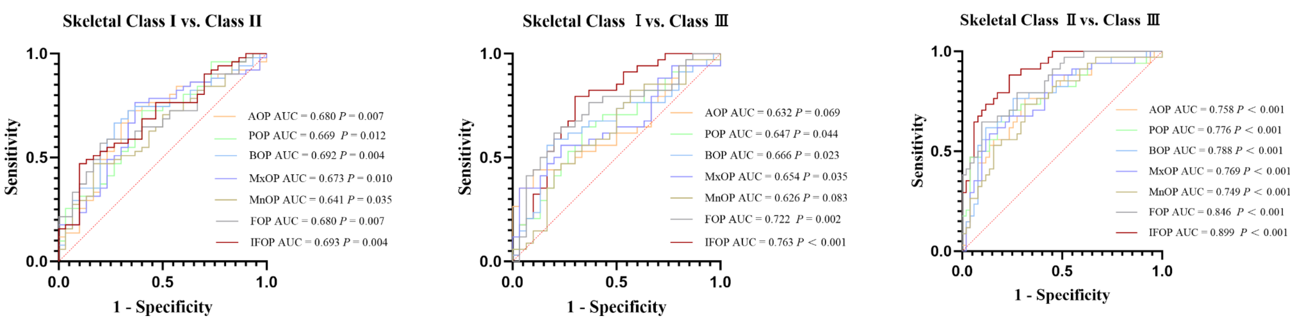

Fig. 5 ROC curves of the inclinations of different OPs for anteroposterior skeletal pattern determinations. OP, Occlusal plane; ROC, Receiver operating characteristic

Table 4 Correlations between inclinations of different occlusal planes (OPs) and APMP metrics

		APDI (°)	ANB (°)	AF-BF (mm)
AOP(°)	*Correlation*	-0.362***	0.327***	0.493***
POP(°)	*Correlation*	-0.433***	0.361***	0.530***
BOP(°)	*Correlation*	-0.414***	0.371***	0.575***
MxOP(°)	*Correlation*	-0.378***	0.326***	0.515***
MnOP(°)	*Correlation*	-0.306***	0.282**	0.450***
FOP(°)	*Correlation*	-0.488***	0.451***	0.679***
IFOP(°)	*Correlation*	-0.557***	0.543***	0.731***

*, *P* value < 0.05; **, *P* value < 0.01; ***, *P* value < 0.001

as the "gold standard" to diagnose the APMP imbalance [43, 44], APDI, ANB, and AF-BF were employed in this study. APDI was selected because of its advantages in small measurement variability [45]. ANB was selected because of its convenience in assessing mandibular relationships only using NA and NB lines [46]. Additionally, we used AF-BF because of its advantages in eliminating the nasion's effect [24]. Undoubtedly, the Wits appraisal is also an important metric for assessing APMP [47]. However, its measurement relies on OP as a reference plane, which exhibited uncertainty and variability in present study; therefore, we did not consider the Wits appraisal in this study.

Many studies have analysed the relationship between OP inclination and APMP [10–13]; however, few have explored the feasibility of OP inclination used in predicting changes in APMP. In the current study, we compared the ability test results of seven OP inclinations in distinguishing different anteroposterior skeletal patterns. The results showed that IFOP inclination had a significantly higher discrimination ability than did the other OP inclinations in skeletal Classes II and III, which indicated the higher feasibility of IFOP inclination used as a parameter in predicting the APMP changes. Furthermore, we also compared the correlation coefficients of inclinations of these OPs to validate the feasibility of IFOP inclination in predicting the APMP changes. These results showed that IFOP inclination, comprising contacted cusps from

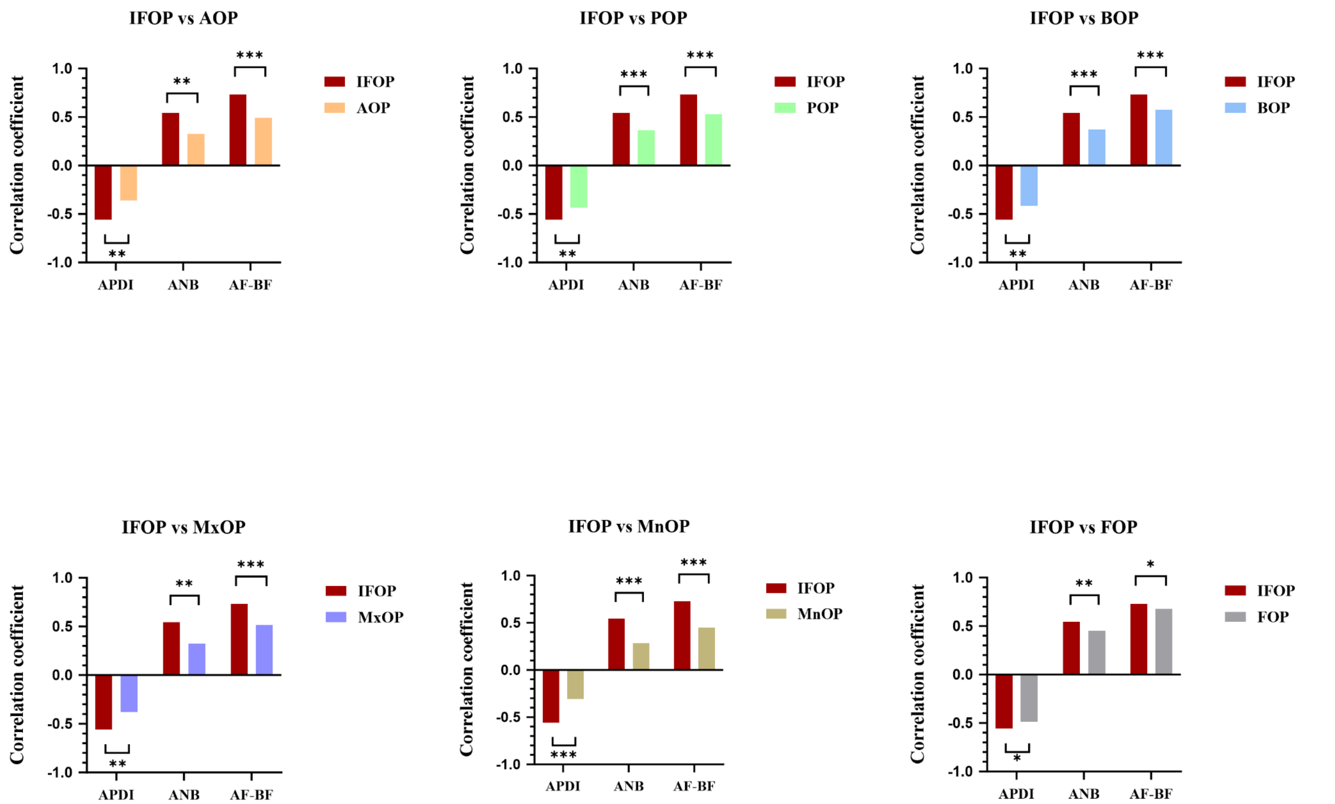

Fig. 6 Correlation coefficients between the inclinations of different OPs and APMP metrics. OP, Occlusal plane; APMP, Anteroposterior mandibular position; *, *P* value < 0.05; **, *P* value < 0.01; ***, *P* value < 0.001

posterior teeth, had the strongest correlation with each APMP metric, and its correlation coefficient with each APMP metric was higher than that of the inclinations of other OPs. The superior performance of IFOP may be attributed to the cusps used used to represent this OP. As is well known, the mandibular condyle is an important growth site in the developing mandible, and is closely associated with maxillofacial skeleton morphogenesis [48, 49]. Mechanical loading is one of the local factors that could affect the growth of condylar cartilage [49, 50]. Differential condylar loading depends on the bite point of the dentition [51]. Therefore, the occlusal contact pattern may significantly contribute to the development of the APMP. Compared with other OPs, the IFOP, constructed by the contacted supporting cusps, more accurately represents the true occlusal contact pattern of the dentition. As a result, it may have a stronger correlation with each APMP metric.

To further explore the effect of the IFOP inclination on the change in each APMP metric, we constructed the regression models of the IFOP inclination and APMP metrics. According to the slope of regression models, the deeper the IFOP inclination, the smaller the APDI, and the greater the ANB and AF-BF. Specifically, the deeper the IFOP inclination, the more retrognathic the mandibular posture. This finding is consistent with that of a study by Coro et al. [12], despite the difference in the focused OP. Nevertheless, we also observed that the IFOP inclination accounted for 32.5%, 31.1%, and 47.4% of the variation in APDI, ANB, and AF-BF, respectively. This suggests that the predictive effect of the IFOP inclination on the changes in each APMP metric is not uniform. Specifically, in predicting changes in APDI and ANB, the effect of IFOP inclination appears to be more limited.

The OP is considered as the "workbench of orthodontics," and the OP inclination is a key parameter need to be focused in the orthodontic treatment [52]. Previous studies have shown that orthodontists can distal en-masse move the dentition or adjust the vertical dimension of dental arches to achieve the control of OP inclination, which leads to the changes of APMP related metrics and improves oral function and facial aesthetics for adult patients with different skeletal malocclusions [53, 54]. Therefore, a quantitative evidence *on* the feasibility and efficiency of OP inclination to predict APMP changes is crucial for achieving the satisfied outcomes in camouflage treatment. The potential clinical applications of this study could be reflected in the identifying specific OP that need to be controlled and predicting changes in APMP metrics. The orthodontist could avoid the unfavorable rotation of mandible by controlling

IFOP inclination during the treatment and develop an appropriate treatment strategy by evaluating the effect of IFOP inclination control on APMP. Considering that orthodontic treatment is oriented toward obtaining an acceptable aesthetic and functional mandibular position for the patient [55, 56], the more predictable of the IFOP inclination on the APMP changes, the better of treatment outcomes.

This study had some limitations. First, we only analysed the OPs formed by the cusps, which may overlook potential contributions from other anatomical structures. Future research will explore the different combinations of OPs and analyse their effect in predicting the changes in APMP. Second, the findings of this study require further clinical validation. In our next study, we will design a cohort study to measure and compare the aesthetic and functional metrics of adult patients with APMP imbalances who receive IFOP control and those who do not, at different stages of orthodontic treatment, to further validate our findings. Finally, the underlying reasons for the superior performance of IFOP than the other OPs need further investigation. Future studies will involve animal experiments and finite element analysis to validate the proposed mechanism.

Conclusion

This study demonstrated that using deep learning-based 3D models to construct the OP formed by the cusps from CBCT data is a feasible approach. Compared with other reported OPs, the IFOP is more suitable to be used as a parameter for predicting APMP changes. Within the range of inclinations that IFOP can achieve, a steeper IFOP inclination corresponded to a more retrognathic mandibular posture.

Abbreviations

3D	Three-dimensional
APDI	Anteroposterior dysplasia indicator
APMP	Anteroposterior mandibular position
AUC	Area under the curve
CBCT	Cone-beam computed tomography
FHP	Frankfort horizontal plane
ICC	Intraclass correlation coefficient
IFOP	Improved functional occlusal plane
OP	Occlusal plane
ROC	Receiver operating characteristic
SRP	Sagittal reference plane

Acknowledgements

Not Applicable.

Author contributions

B.D. conducted the investigation, methodology, and original draft preparation. K.L. handled software development, validation, and investigation. Z.S. was responsible for writing the original draft and formal analysis. Y.C. contributed to measurement and formal analysis. J.Y., Y.P., and Z.H. managed data curation and investigation. F.H. oversaw project administration. X.R.F. reviewed and edited the draft. Y.Z. worked on software, visualization, and methodology. X.Z. provided resources, supervision, and conceptualization. All authors have read and approved the final manuscript.

Funding

This work was supported by the Key Fields Special Project of Guangdong Universities (2021ZDZX1024), Foshan Engineering Technology Research Center for Oral Functional Occlusion Reconstruction of Periodontal Disease (GCJSYJZX2024-008), Guangdong Basic and Applied Basic Research Foundation (2024A1515010413), and the 2023 Provincial College Student Innovation and Entrepreneurship Training Program of Southern Medical University (S202312121171).

Data availability

The datasets used and/or analysed during the current study are available from the corresponding author on reasonable request.

Declarations

Ethics approval and consent to participate

All patients provided informed consents to participate in this study, and the study was approved by the Research Ethics Commission of the Department of Stomatology, Shunde Hospital, Southern Medical University (Approval No.: KYLS20220913). All procedures of this study were performed in accordance with the relevant guidelines and regulations.

Consent for publication

Not applicable.

Competing interests

The authors declare no competing interests.

Author details

[1]Department of Stomatology, Shunde Hospital, Southern Medical University (The First People's Hospital of Shunde, Foshan), Foshan 528308, Guangdong, China
[2]School of Mathematics, South China University of Technology, Guangzhou 510641, Guangdong, China
[3]Stomatological Hospital, School of Stomatology, Southern Medical University, Guangzhou 510280, Guangdong, China
[4]Center of Clinic Research, Division of Conservative Dentistry and Periodontology, University Dental Clinic, Medical University Vienna, Vienna 1090, Austria

Received: 5 October 2024 / Accepted: 13 December 2024
Published online: 08 January 2025

References

1. Buschang PHP, Jacob HBDP. Mandibular rotation revisited: what makes it so important? Semin Orthod. 2014;20:299–315.
2. Kim KM, Sasaguri K, Akimoto S, Sato S. Mandibular rotation and occlusal development during facial growth. Int J Stomatol Occlusion Med. 2009;2:122–30.
3. Sasaki Y, Yamamoto JI, Kanzaki H, Shimpo Y, Miyamoto Y, Kobayashi F, et al. Association between severity of malocclusion and parameters of oral functions in permanent dentition with various malocclusion: case-control study. Clin Investig Orthod. 2023;82:212–21.
4. Guo R, Tian Y, Li X, Li W, He D, Sun Y. Facial profile evaluation and prediction of skeletal class II patients during camouflage extraction treatment: a pilot study. Head Face Med. 2023;19:51.
5. Silvola AS, Närhi L, Tolvanen M, Pirttiniemi P. Gender-specific associations of malocclusion traits with oral health-related quality of life in a Finnish adult population. Eur J Orthod. 2020;42:242–9.
6. Ardani IGAW, Wicaksono A, Hamid T. The occlusal plane inclination analysis for determining skeletal Class III malocclusion diagnosis. Clin Cosmet Investig Dent. 2020;12:163–71.
7. Park JH, Yu J, Bullen R. Camouflage treatment of skeletal Class III malocclusion with conventional orthodontic therapy. Am J Orthod Dentofac Orthop. 2017;151:804–11.
8. Wang Y, Zhou Y, Zhang J, Wang X. Long-term stability of counterclockwise mandibular rotation by miniscrew-assisted maxillary intrusion in adult patients with skeletal Class II high-angle malocclusion: a 10-year follow-up of 2 patients. AJO-DO Clin Companion. 2022;2:601–17.

9. Li JL, Kau CH, Wang M. Changes of occlusal plane inclination after orthodontic treatment in different dentoskeletal frames. Prog Orthod. 2014;15:41.
10. Bushra E. Variations in the human facial pattern in norma lateralis. Angle Orthod. 1948;18:100–2.
11. Fushima K, Kitamura Y, Mita H, Sato S, Suzuki Y, Kim YH. Significance of the cant of the posterior occlusal plane in class II division 1 malocclusions. Eur J Orthod. 1996;18:27–40.
12. Coro JC, Velasquez RL, Coro IM, Wheeler TT, McGorray SP, Sato S. Relationship of maxillary 3-dimensional posterior occlusal plane to mandibular spatial position and morphology. Am J Orthod Dentofac Orthop. 2016;150:140–52.
13. Ye R, Li Y, Li X, Li J, Wang J, Zhao S, Zhao Z. Occlusal plane canting reduction accompanies mandibular counterclockwise rotation in camouflaging treatment of hyperdivergent skeletal Class II malocclusion. Angle Orthod. 2013;83:758–65.
14. Kuroda S, Katayama A, Takano-Yamamoto T. Severe anterior open-bite case treated using titanium screw anchorage. Angle Orthod. 2004;74:558–67.
15. He Y, Wang Y, Wang X, Wang J, Bai D, Guo Y. Nonsurgical treatment of a hyperdivergent skeletal Class III patient with mini-screw-assisted mandibular dentition distalization and flattening of the occlusal plane. Angle Orthod. 2022;92:287–93.
16. Wen J, Liu S, Ye X, Xie X, Li J, Li H, et al. Comparative study of cephalometric measurements using 3 imaging modalities. J Am Dent Assoc. 2017;148:913–21.
17. Kapila SD, Nervina JM. CBCT in orthodontics: assessment of treatment outcomes and indications for its use. Dentomaxillofac Radiol. 2015;44:20140282.
18. Cui Z, Fang Y, Mei L, Zhang B, Yu B, Liu J, et al. A fully automatic AI system for tooth and alveolar bone segmentation from cone-beam CT images. Nat Commun. 2022;13:2096.
19. Elgarba BM, Van Aelst S, Swaity A, Morgan N, Shujaat S, Jacobs R. Deep learning-based segmentation of dental implants on cone-beam computed tomography images: a validation study. J Dent. 2023;137:104639.
20. Verhelst PJ, Smolders A, Beznik T, Meewis J, Vandemeulebroucke A, Shaheen E, et al. Layered deep learning for automatic mandibular segmentation in cone-beam computed tomography. J Dent. 2021;114:103786.
21. Imamura K, Terajima M, Nakashima A, Takahashi I. A three-dimensional analysis of masticatory muscles in laterognathism. Orthod Waves (English ed). 2019;78:143–50.
22. Freudenthaler J, Celar A, Kubota M, Akimoto S, Sato S, Schneider B. Comparison of Japanese and European Overbite Depth Indicator and Antero-Posterior Dysplasia Indicator Values. Eur J Orthod. 2012;34:114–8.
23. Riedel RA. The relation of maxillary structures to cranium in malocclusion and in normal occlusion. Angle Orthod. 1952;22:140–45.
24. Chang HP. Assessment of anteroposterior jaw relationship. Am J Orthod Dentofac Orthop. 1987;92:117–22.
25. Laquihuanaco G, Rodríguez-Cárdenas Y, Ruíz-Mora G, Meneses-López A, Arriola-Guillén L. Mandibular angle morphology in open bite subjects according to the skeletal relationship: a cbct short report. J Oral Res. 2022;11:1–12.
26. Dot G, Rafflenbeul F, Kerbrat A, Rouch P, Gajny L, Schouman T. Three-dimensional cephalometric landmarking and Frankfort horizontal plane construction: reproducibility of conventional and novel landmarks. J Clin Med. 2021;10:5303.
27. Pittayapat P, Jacobs R, Bornstein MM, Odri GA, Lambrichts I, Willems G, et al. Three-dimensional Frankfort horizontal plane for 3D cephalometry: a comparative assessment of conventional versus novel landmarks and horizontal planes. Eur J Orthod. 2018;40:239–48.
28. Green MN, Bloom JM, Kulbersh R. A simple and accurate craniofacial midsagittal plane definition. Am J Orthod Dentofac Orthop. 2017;152:355–63.
29. Abate A, Cavagnetto D, Lanteri V, Maspero C. Three-dimensional evaluation of the maxillary sinus in patients with different skeletal classes and cranio-maxillary relationships assessed with cone beam computed tomography. Sci Rep. 2023;13:2098.
30. Hassan B, Nijkamp P, Verheij H, Tairie J, Vink C, van der Stelt P, et al. Precision of identifying cephalometric landmarks with cone beam computed tomography in vivo. Eur J Orthod. 2013;35:38–44.
31. Velásquez RL, Coro JC, Londoño A, McGorray SP, Wheeler TT, Sato S. Three-dimensional morphological characterization of malocclusions with mandibular lateral displacement using cone-beam computed tomography. Cranio. 2018;36:143–55.
32. Nelvi Yohana SBAN. The changing of occlusal plane inclination in Class II malocclusion. Dent J. 2020;53:133–9.
33. Moshiri S, Araújo EA, McCray JF, Thiesen G, Kim KB. Cephalometric evaluation of adult anterior open bite non-extraction treatment with Invisalign. Dent Press J Orthod. 2017;22:30–8.
34. Chan HJ, Woods M, Stella D. Mandibular muscle morphology in children with different vertical facial patterns: a 3-dimensional computed tomography study. Am J Orthod Dentofac Orthop. 2008;133:10–1.
35. Teng C, Zhong T, Yu Q. Relationships between jaw deformity and the occlusal plane in cone beam computed tomography scans. J Prosthet Dent. 2022;128:49–54.
36. Meng XL, Rosenthal R, Rubin DB. Comparing correlated correlation coefficients. Psychol Bull. 1992;111:172–5.
37. Koo TK, Li MY. A guideline of selecting and reporting intraclass correlation coefficients for reliability research. J Chiropr Med. 2016;15:155–63.
38. Kim H. Statistical notes for clinical researchers: evaluation of measurement error 2: Dahlberg's error, Bland-Altman method, and Kappa coefficient. Restor Dent Endod. 2013;38:182.
39. Osnes CA, Wu JH, Venezia P, Ferrari M, Keeling AJ. Full arch precision of six intraoral scanners in vitro. J Prosthodont Res. 2019;64:6–11.
40. Winkler J, Gkantidis N. Trueness and precision of intraoral scanners in the maxillary dental arch: an in vivo analysis. Sci Rep. 2020;10:1172.
41. Mangano F, Gandolfi A, Luongo G, Logozzo S. Intraoral scanners in dentistry: a review of the current literature. BMC Oral Health. 2017;17:149.
42. Hung KF, Ai QYH, Wong LM, Yeung AWK, Li DTS, Leung YY. Current applications of deep learning and radiomics on CT and CBCT for maxillofacial diseases. Diagnostics (Basel). 2023;13:110.
43. Han UK, Kim YH. Determination of Class II and Class III skeletal patterns: receiver operating characteristic (ROC) analysis on various cephalometric measurements. Am J Orthod Dentofac Orthop. 1998;113:538–45.
44. Sheikh ZN, Mohammad M. A comparative evaluation of ANB angle with other linear cum angular skeletal and occlusal parameters in different sagittal dysplasias. Int J Appl Dent Sci. 2020;6:459–64.
45. Oktay H. A comparison of ANB, WITS, AF-BF, and APDI measurements. Am J Orthod Dentofac Orthop. 1991;99:122.
46. Cecil C, Steiner DDS. Cephalometrics for you and me. Am J Orthod. 1953;39:729–55.
47. Jacobson A. The Wits appraisal of jaw disharmony. Am J Orthod. 1975;67:125–38.
48. Mizoguchi I, Toriya N, Nakao Y. Growth of the mandible and biological characteristics of the mandibular condylar cartilage. Jpn Dent Sci Rev. 2013;49:139–50.
49. Von den Hoff JW, Delatte M. Interplay of mechanical loading and growth factors in the mandibular condyle. Arch Oral Biol. 2008;53:709–15.
50. Ng AF, Yang YO, Wong RW, Hägg EU, Rabie AB. Factors regulating condylar cartilage growth under repeated load application. Front Biosci. 2006;11:949–54.
51. Peck CC. Biomechanics of occlusion – Implications for oral rehabilitation. J Oral Rehabil. 2016;43:205–14.
52. Lamarque S. The importance of occlusal plane control during orthodontic mechanotherapy. Am J Orthod Dentofac Orthop. 1995;107:548–58.
53. Jing Y, Han X, Guo Y, Li J, Bai D. Nonsurgical correction of a Class III malocclusion in an adult by miniscrew-assisted mandibular dentition distalization. Am J Orthod Dentofac Orthop. 2013;143:877–87.
54. Li X, Zhao Q, Zhao R, Gao M, Gao X, Lai W. Effect of occlusal plane control procedure on hyoid bone position and pharyngeal airway of hyperdivergent skeletal Class II patients. Angle Orthod. 2017;87:293–99.
55. Turley PK. Evolution of esthetic considerations in orthodontics. Am J Orthod Dentofac Orthop. 2015;148:374–9.
56. Perry JHT. Mandibular function: an orthodontic responsibility. Am J Orthod. 1975;67:316.

Publisher's note